2013-07-18

A Guiding Potential Method for Evaluating the Bending Rigidity of Tensionless Lipid Membranes from Molecular Simulation

UTD AUTHOR(S): Stephen O. Nielsen

A guiding potential method for evaluating the bending rigidity of tensionless lipid membranes from molecular simulation

Shuhei Kawamoto, Takenobu Nakamura, Steven O. Nielsen, and Wataru Shinoda

Citation: The Journal of Chemical Physics **139**, 034108 (2013); doi: 10.1063/1.4811677
View online: http://dx.doi.org/10.1063/1.4811677
View Table of Contents: http://scitation.aip.org/content/aip/journal/jcp/139/3?ver=pdfcov
Published by the AIP Publishing

A guiding potential method for evaluating the bending rigidity of tensionless lipid membranes from molecular simulation

Shuhei Kawamoto,[1,a)] Takenobu Nakamura,[2] Steven O. Nielsen,[3] and Wataru Shinoda[1,b)]
[1]*National Institute of Advanced Industrial Science and Technology (AIST), 1-8-31 Midorigaoka, Ikeda, Osaka 563-8577, Japan*
[2]*Advanced Institute for Materials Research, Tohoku University, 2-1-1 Katahira Aoba-ku, Sendai, Miyagi 980-8577, Japan*
[3]*Department of Chemistry, The University of Texas at Dallas, 800 West Campbell Road, Richardson, Texas 75080, USA*

(Received 7 March 2013; accepted 5 June 2013; published online 18 July 2013)

A new method is proposed to estimate the bending rigidity of lipid membranes from molecular dynamics simulations. An external cylindrical guiding potential is used to impose a sinusoidal deformation to a planar membrane. The bending rigidity is obtained from the mean force acting on the cylinder by calibrating against a discretized Helfrich model that accounts for thermal fluctuations of the membrane surface. The method has been successfully applied to a dimyristoyl phosphatidylcholine bilayer simulated with a coarse-grained model. A well-converged bending rigidity was obtained for the tension-free membrane and showed reasonable agreement with that obtained from the height fluctuation spectrum. © *2013 AIP Publishing LLC*. [http://dx.doi.org/10.1063/1.4811677]

I. INTRODUCTION

Lipid membranes show fascinating morphologies owing to their fluidity and flexibility. The membrane morphologies can be conventionally described by the Helfrich model,[1] which uses a quadratic curvature expansion of the free energy:

$$E = \int dS \left(\frac{\kappa}{2}(c_1 + c_2 - c_0)^2 + \bar{\kappa} c_1 c_2 \right). \tag{1}$$

Here c_1 and c_2 are the principal curvature radii of the membrane surface and the integral is over the total area of the membrane. κ is the bending rigidity, $\bar{\kappa}$ is the saddle-splay modulus, and c_0 is the spontaneous curvature. In spite of its simplicity, the model has been successfully used to characterize various membrane morphologies observed experimentally.

The elastic parameters depend on the composition of the lipid membrane. For example, the bending rigidity is affected by the concentration of cholesterol,[2,3] the length and unsaturation of the lipid tail alkyl chains,[4] and the presence HIV-1 fusion peptide.[5] Thus, a link between the elastic parameters and the molecular components of the membrane should provide a useful way to predict the mesoscopic, elastic behavior of the membrane from the viewpoint of molecular science. Therefore, many theoretical and simulation studies have been undertaken to evaluate the elastic parameters using molecular dynamics (MD) simulation trajectories.[6,7] The saddle-splay modulus and the spontaneous curvature are often estimated by using the stress profile across the membrane.[8–12]

To calculate the bending rigidity from MD simulations, several different methods have been proposed. The most commonly used method is based on the height fluctuation spectrum of a membrane.[13–20] An equilibrated MD trajectory of a planar lipid bilayer, of infinite extent due to the use of periodic boundary conditions (PBC), is employed for the analysis. The height fluctuation spectrum $\langle |h_q|^2 \rangle$ is derived from the Helfrich model

$$\langle |h_q|^2 \rangle = \frac{k_B T}{q^4 \kappa}, \tag{2}$$

where $q = 2\pi n/L$ is the wavenumber, k_B is the Boltzmann constant, T is temperature, and L is the box size. $\langle \cdots \rangle$ denotes the ensemble average. By fitting a height fluctuation spectrum measured from MD simulations to this expression, we obtain the bending rigidity κ. Since the Helfrich model considers an elastic membrane with zero thickness, Eq. (2) should be most accurate in the limit of $q \to 0$. However, the convergence of the low-q modes is slower than that of the high-q modes simply because of the available data density from MD trajectories. In addition, it was recently pointed out that uncertainty in the choice of cutoff frequency, q_{cut}, for the fitting may cause a serious error.[20] To minimize the fitting error, an elastic Hamiltonian for membrane energetics that captures bilayer undulations and peristaltic deformations over all wavelengths was proposed and used to estimate the elastic parameters.[21] However, the intrinsic problem of the slow convergence of important low-q modes still remains, so that substantial sampling is required to be able to resolve the spectrum.

Recently, a new approach to estimate the bending rigidity using thermal fluctuations of lipid orientation has been proposed.[22] The method is based on a fluctuation analysis of an equilibrated membrane, and has a significant advantage in better convergence at shorter wavelengths. Thus, the method allows us to use a MD trajectory of a modest system size for estimating the bending rigidity without a serious fitting error. A few test calculations for DMPC bilayers with different force fields indeed demonstrated a good numerical nature of the spectrum of longitudinal molecular orientation fluctuations,

a)Electronic mail: s.kawamoto@aist.go.jp
b)Electronic mail: w.shinoda@aist.go.jp

though the estimated bending rigidity seems systematically larger than that obtained from the standard height fluctuation spectrum.[22]

Apart from fluctuation analysis, a more intuitive method is to measure the bending rigidity from a response (force) of a deformed membrane. den Otter and Briels[27] invented a method to measure the mean force required to impose a sinusoidal deformation to a lipid membrane. This method uses the amplitude of selected undulatory modes as a reaction coordinate and evaluates the mean force to keep the membrane at the target amplitude. The calculated mean force was compared to that predicted from the Helfrich Hamiltonian to deduce the bending rigidity. This method was elegantly formulated, though a practical problem remains in the slow convergence of the bending rigidity. Farago and Pincus proposed a different method by considering the free energy required to deform the membrane.[23] Even though their approach could investigate the relation between a microscopic expression and elastic coefficients, the numerical convergence of the bending rigidity seems to be worse than that in the height fluctuation spectrum.[23] Therefore, these methods have not been widely used in practical simulations of realistic membrane models.

Harmandaris and Deserno used a tubular membrane spanning the simulation box to evaluate the bending rigidity.[24] The imposed curvature of the tubular geometry is advantageous for evaluating the bending energy, which generates a net pulling force along the axial direction of the tube. The force is detected as a pressure difference between the axial and radial directions. The bending rigidity, κ, is estimated from the relationship $F = 2\pi\kappa/R$, where F is the force and R is the radius of the tube. The method was successfully applied to a simple coarse-grained (CG) model.[24] A problem arises, however, when we apply the method to a realistic molecular model because of the difficulty of preparing a strain-free initial configuration of the tubular membrane. A flip-flop motion is prohibitively rare in a bilayer simulation using a realistic model so that the number of lipids in each leaflet has to be carefully chosen to realize a relaxed tubular membrane.

The method proposed by den Otter,[25] and later separately by Noguchi,[26] applies a lateral compression to a planar membrane under PBC. When the compression exceeds a threshold value, the membrane buckles. The bending rigidity is calculated from a relation between the curvature of the membrane and the lateral force needed to support the buckled membrane. Even though the curvature has been changed owing to the lateral compression, the two leaflets of the bilayer are symmetrically curved so that the bilayer can be relaxed without an exchange of lipids. This is advantageous over the tubular membrane method for application to a realistic membrane model. However, the bending rigidity obtained in this way is for the laterally compressed membrane, which may not be the same as that of the tensionless membrane.

In this work, we propose a novel method to estimate the bending rigidity of lipid membranes from a MD simulation in which external guiding potentials are added to the standard force field. Two cylindrical guiding potentials are employed to impose a sinusoidal deformation to a planar membrane (see Fig. 1). We measure the restoring force of the deformed membrane, which is detected as the mean force exerted on the membrane from the cylinders. The mean force is determined as a function of the curvature of the deformed membrane and the bending rigidity through the Helfrich model. We numerically solve the Helfrich model, which provides reference data to estimate the bending rigidity by a measurement of the mean force from a MD simulation. The bending rigidity obtained in this way shows good agreement with that estimated by the height fluctuation spectrum of the tensionless membrane.

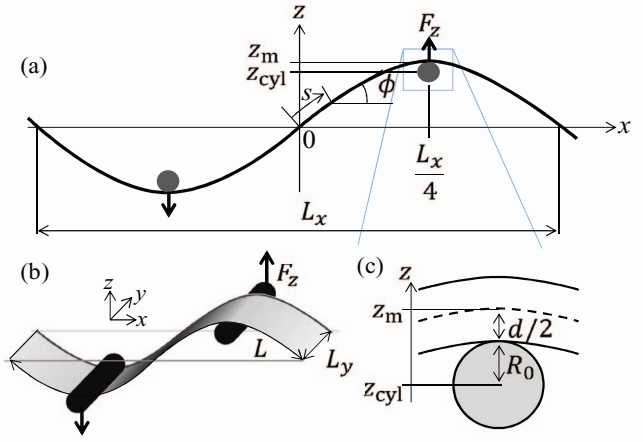

FIG. 1. The membrane bends in the x-direction under the influence of two cylinders with their long axis along the y-direction. (a) Schematic of the deformed surface projected onto the xz plane. Two filled circles represent the cylinders. (b) The 3D image of panel (a). (c) Closeup view near one of the cylinders. The membranes described in MD simulations have a finite thickness of d whereas the thickness is zero in the Helfrich model.

Among the previously available methods, the present guiding method is most closely related to the method by den Otter and Briels.[27] Both measure the mean force required to impose a sinusoidal deformation to the membrane, and obtain the bending rigidity by a comparison of the force estimated from the Helfrich model. However, the present method has a significant advantage in the numerical precision of the obtained bending rigidity. One of the most important differences is that the present method evaluates the force required for the deformation of the Helfrich membrane numerically, rather than analytically, without using a small gradient approximation. In the previous method,[27] due to the small gradient approximation, the amplitude of membrane deformations was limited in the small amplitude range. Therefore, the required force to impose the bending cannot be large compared to the thermal noise. This, in practice, limits the numerical precision for the estimation of the bending rigidity. Also, the previous method[27] deforms the membrane under constant volume conditions, while the present method employs constant pressure conditions (NPT ensemble), which can more naturally simulate a tension free membrane. Because the overall deformation of the two leaflets of the bilayer is identical in the present method, the structural relaxation should occur without exchange of lipids between the two leaflets, that is, no flip-flop motion is required in contrast to the case of the tubular membrane.[24] Unlike the lateral compression method, here the membrane curvature is directly changed due to the external field. Therefore, the net tension is kept negligibly small in the NPT ensemble as long as the deformation of the membrane

is small. Thus, we can evaluate the bending rigidity of a tensionless membrane using the present method.

The remainder of this paper is organized as follows. In Sec. II, we derive a relation between the bending rigidity and the force required for the membrane deformation using the Helfrich model. The relation was numerically solved using a Langevin dynamics (LD) simulation of the discretized version of the Helfrich model to take into account the thermal fluctuations of the membrane. The details of the molecular model and the molecular dynamics simulations are also provided. Furthermore, we briefly explain how we calculate the spectrum of thermal fluctuations of height and lipid orientation, respectively, and applied the lateral compression method[25,26] in the context of our MD simulations, which were used for a comparison to our numerical simulations. In Sec. III, simulation results are presented for both the Helfrich and coarse-grained molecular models. Using a dimyristoyl phosphatidylcholine (DMPC) bilayer as a test system, we demonstrate that the present method yields a reasonable bending rigidity. The paper ends with conclusions in Sec. IV.

II. METHODS

A. Normal force required to support membrane curvature

We consider a symmetric lipid bilayer with zero spontaneous curvature. The membrane undergoes a sinusoidal deformation in the x-direction due to the influence of two cylinders placed as shown in Fig. 1. If we can measure the force required for the deformation as a function of the induced curvature, we can evaluate the bending rigidity of the membrane using the Helfrich model (or more generally a stress-strain relation).

In this section, we first derive a formal expression for the force required to support an ideally deformed membrane from the Helfrich model, and then give a discretized membrane model to numerically evaluate the bending rigidity based on the Helfrich model. The latter is introduced to include the effect of thermal fluctuations in the force calculation. Finally, we give the simulation conditions together with the details of the model system.

1. Helfrich model

Suppose a lipid membrane spans the simulation unit cell in the L_x and L_y directions under PBC. As shown in Fig. 1, the membrane is curved only along L_x, so that the membrane curvature along L_y is roughly zero. The box size L_y is held fixed and L_x is adjusted to realize zero surface tension. We ignore the increase of surface tension along L_y due to the anisotropy of the curved membrane,[26] which should be reasonable as long as the membrane curvature is not too large. We also assume that the intrinsic area of the membrane is kept constant at $S = L \times L_y$ during this deformation. Here L is the length of the membrane measured along the membrane surface in the x-direction. The energy change for the membrane deformation is then written as[26]

$$E_{\mathrm{bend}}[\phi] = \frac{\kappa L_y}{2} \int_0^L ds \left(\frac{d\phi}{ds}\right)^2, \tag{3}$$

where κ is the bending rigidity. In this expression, the bending energy is simply described by the arc length, s, and the angle ϕ between the tangent line and the x-axis (see Fig. 1(a)). We assume the interval between the two cylinders is shorter than the persistence length of the membrane, so that the membrane behaves ideally as an elastic sheet touching each cylinder at points in the xz plane: $(x, z) = (L_x/4, z_{\mathrm{m}})$ and $(-L_x/4, -z_{\mathrm{m}})$. From symmetry, we can write this condition simply as

$$\int_0^{L/4} ds \sin\phi = z_{\mathrm{m}}. \tag{4}$$

The membrane shape is determined by minimizing the bending energy E_{bend} under the condition of Eq. (4). The Euler-Lagrange equation is written as

$$-\lambda \cos\phi + \frac{d^2\phi}{ds^2} = 0, \tag{5}$$

where λ is the Lagrange multiplier. According to the symmetry of the deformation, the equation is solved with the following boundary conditions:

$$\phi\left(\frac{L}{4}\right) = 0, \tag{6}$$

$$\left.\frac{d\phi}{ds}\right|_{s=0} = 0. \tag{7}$$

Using the solution of Eq. (5), $\phi = \phi^*$, we obtain the bending energy as a function of z_{m}. The derivative of the bending energy with respect to z_{m} yields the restoring force at the point $(L_x/4, z_{\mathrm{m}})$ along the z-axis

$$F_{z\mathrm{H}} = -\frac{1}{2}\frac{\partial E_{\mathrm{bend}}[\phi^*]}{\partial z_{\mathrm{m}}}, \tag{8}$$

where the factor of 1/2 is included to account for the two cylinders in the simulation box. In the small bending regime limit, $z_{\mathrm{m}}/L \ll 1$, the force is derived as

$$F_{z\mathrm{H}} = 96\kappa \frac{L_y z_{\mathrm{m}}}{L^3}. \tag{9}$$

2. Discretized Helfrich model with external cylindrical potential

Here we introduce a discrete particle model that is designed to reproduce the elastic behavior of the Helfrich model. Even though the force has to be evaluated numerically using the discretized model, we can explicitly consider the thermal fluctuations of the membrane. The membrane deformation is applied by an explicit consideration of the cylindrical guiding potentials rather than as a boundary condition of Eq. (4). This is advantageous for a comparison with the MD simulations as discussed later.

The model describes the membrane with n bead segments: $\int_0^L ds \to \sum_{i=1}^n \Delta s$, where $\Delta s = L/n$. Then, we

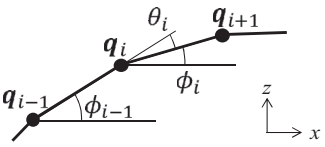

FIG. 2. Definition of angles θ_i in the discrete particle model of the membrane.

rewrite the bending energy as follows:

$$\begin{aligned} E_{\text{bend}} &= \frac{\kappa L_y}{2}\int_0^L ds\left(\frac{d\phi}{ds}\right)^2 \\ &\simeq \frac{\kappa L_y}{2}\frac{L}{n}\sum_{i=1}^{n}\left(\frac{\phi_i-\phi_{i-1}}{\Delta s}\right)^2 \\ &= \sum_{i=1}^{n}\frac{1}{2}\frac{n\kappa L_y}{L}\theta_i^2 \\ &= \sum_{i=1}^{n}\frac{1}{2}k_\theta\theta_i^2. \end{aligned} \tag{10}$$

Here $k_\theta \equiv n\kappa L_y/L$, ϕ_i is the tangential angle at segment i, and $\theta_i = \phi_i - \phi_{i-1}$, as shown in Fig. 2. $\theta_0 = \theta_n$ because of PBC. The bond length between the neighboring segments should be kept at Δs. This is in principle feasible using the SHAKE algorithm.[28] For the sake of computational simplicity, however, we instead introduce a harmonic potential to keep the bond length close to Δs:

$$U_{\text{bond}} = \sum_{i=1}^{n}\frac{1}{2}k_{\text{bond}}(|\boldsymbol{q}_i - \boldsymbol{q}_{i+1}| - \Delta s)^2, \tag{11}$$

where $\boldsymbol{q}_i = (x_i, z_i)$ is the position of ith bead. We need to consider the effect of the strength of the bond force constant on the simulation results. The spring constant, k_{bond}, should be changed depending on n, κ and the membrane size L, L_y. It is convenient to use a dimensionless parameter, k^*_{bond}, to control the stiffness of the bond potential

$$k^*_{\text{bond}} = k_{\text{bond}}\frac{L^3}{n\kappa L_y}. \tag{12}$$

We find that $k^*_{\text{bond}} = 6.4\times10^4$ is large enough to obtain a well converged result as shown later.

We now consider the cylindrical wall potential used to impose the membrane bending. As shown in Fig. 1, two cylindrical potentials U_+ and U_- are placed at $(L_x/4, z_c)$ and $(-L_x/4, -z_c)$, respectively, pushing the membrane in opposite directions along the z-axis:

$$U_{\text{cylinder}} = \sum_{i=1}^{n}(u_+(\boldsymbol{q}_i) + u_-(\boldsymbol{q}_i)). \tag{13}$$

We choose a purely repulsive cylindrical wall potential for $u_\pm$:

$$u_\pm(\boldsymbol{q}_i) = \begin{cases} -\frac{k_{\text{cyl}}}{3}\Delta R_\pm(\boldsymbol{q}_i)^3 & \text{for } \Delta R_\pm(\boldsymbol{q}_i) < 0 \\ 0 & \text{for } \Delta R_\pm(\boldsymbol{q}_i) \geq 0 \end{cases}, \tag{14}$$

where

$$\Delta R_\pm(\boldsymbol{q}_i) = \sqrt{\left(x_i \mp \frac{L_x}{4}\right)^2 + (z_i \mp z_c)^2} - R_0. \tag{15}$$

Thus, for a large k_{cyl} value, beads are expelled from the cylinder interior. The force exerted on the membrane from the cylinders is calculated by

$$F_{zH\pm} = -\left\langle\sum_{i=1}^{n}\frac{\partial u_\pm}{\partial z_i}\right\rangle, \tag{16}$$

where $\langle\cdots\rangle$ denotes an ensemble average, and z_i is the z-coordinate of the ith bead. These two force components should have the same magnitude but opposite sign. Therefore, for sampling efficiency, we take the average of the forces exerted on the two cylinders:

$$F_{z\text{H}} = \frac{|F_{zH+}| + |F_{zH-}|}{2}, \tag{17}$$

which should be comparable to Eq. (8).

We evaluate the averaged force for each fixed position of the cylinder, z_{m}, during a numerical simulation of the system of a chain of n connected particles, which is described by the potential energy $U = E_{\text{bend}} + U_{\text{bond}} + U_{\text{cylinder}}$. We used a LD simulation to thermalize the system and evaluate the average force in Eq. (16). The equation of motion (EOM) of the ith particle is given in the xz plane as

$$m\frac{d^2\boldsymbol{q}_i}{dt^2} = -\frac{\partial U}{\partial \boldsymbol{q}_i} - \gamma\frac{d\boldsymbol{q}_i}{dt} + \sqrt{\gamma k_{\text{B}}T}\boldsymbol{\zeta}_i, \tag{18}$$

where m is the mass of particle, γ is the friction coefficient, and $\boldsymbol{\zeta}_i$ is zero-mean Gaussian white noise satisfying the condition

$$\langle\zeta_{i\alpha}(t)\zeta_{j\beta}(t')\rangle = 2\delta_{\alpha\beta}\delta_{ij}\delta(t-t'), \tag{19}$$

where α and β are indices for the x and z axis, respectively. The system is also coupled to a Parrinello-Rahman barostat[29] to realize a zero tension in the x-direction. The simulation setup is chosen to represent a membrane similar to the molecular system described in the next subsection, namely, $T = 310$ K and $L_y = 6.3$ nm, which is used to determine the bending constant k_θ, and $L/L_y = 1$–6. The radius and force constant of the cylinder are $R_0 = 0.6$ nm and $k_{\text{cyl}} = 41\,840$ kJ/mol/nm^3. The specific parameters for the LD simulations of the discretized Helfrich model are as follows. The discretization number is $n = 64$; the time step used to integrate the EOM is 0.005τ; the friction coefficient is $\gamma = 1.0m/\tau$; and the time constant for the pressure control is $\tau_p = 10\tau$. The LD simulation length at each sampling point is $10\,000\tau$. τ is the fundamental unit of time, $9(L/n)^2(\rho/\kappa)^{1/2}$, where $\rho = 2186$ amu/nm^2 is the density of the membrane. The mass of the particle is $m = \rho LL_y/n$. We have carried out the LD simulations in the range of $\kappa = (1$–$20)\times10^{-20}$ J to obtain the average force $F_{z\text{H}}$ as a function of z_{m}, which is later used as reference data to determine the bending rigidity of the molecular system from MD simulations.

3. Molecular dynamics simulation

We have employed a coarse grained molecular model to simulate a DMPC bilayer system.[30,31] In this model, a single CG water particle represents three water molecules, and a DMPC molecule is described using 13 connected CG segments. Eight of the 13 segments are hydrophobic denoted as CM and CT. CT represents a terminal alkane group of $CH_3CH_2CH_2-$ and CM represents $-CH_2CH_2CH_2-$. For further details, we refer the reader to the original papers.[30,31]

The external cylinder potential is introduced in a similar manner as shown in Fig. 1, though only the CT and CM segments interact with the cylinders

$$U^{\mathrm{CG}}_{\mathrm{cylinder}} = \sum_{i\in \mathrm{CM,CT}} \left(u_+(\boldsymbol{r}_i) + u_-(\boldsymbol{r}_i)\right), \tag{20}$$

where $\boldsymbol{r}_i = (x_i, y_i, z_i)$ denotes the coordinate of the ith CG segment. The same repulsive potential is used as given in Eqs. (14) and (15), which should be read by replacing $\boldsymbol{q}$ by $\boldsymbol{r}$. Thus, this potential excludes only DMPC hydrophobic chains from the cylindrical region, while water and hydrophilic segments (lipid head groups) have free access to this region. We use the same k_{cyl} and R_0 as in the LD simulations of the discretized Helfrich model. The simulation results are not sensitive to the choice of these parameters, although $R_0 = 0.6$ nm should be smaller than the radius of the membrane curvature and should be larger than individual lipid molecules to support the membrane. The forces exerted on the membrane (the molecular system) from the two cylinders are calculated as

$$F_{z\mathrm{CG}\pm} = -\left\langle \sum_{i\in \mathrm{CM,CT}} \frac{\partial u_\pm}{\partial z_i} \right\rangle. \tag{21}$$

These two force components should have the same magnitude but opposite sign. As in Eq. (17), we take the average of these forces to compare with the Helfrich model of Eq. (17):

$$F_{z\mathrm{CG}} = \frac{|F_{z\mathrm{CG}+}| + |F_{z\mathrm{CG}-}|}{2}. \tag{22}$$

Unlike the Helfrich model, we need to evaluate the membrane thickness, d, to define the mid-plane position, z_{m}, as depicted in Fig. 1(c):

$$z_{\mathrm{m}} = z_{\mathrm{cyl}} + R_0 + \frac{d}{2}, \tag{23}$$

where the cylinder position along the z-axis, z_{cyl}, and the cylinder radius, R_0, are given parameters. Here we define the positive direction of z_{m} and z_{cyl} to point towards the membrane. We determine d using the linear relation between the force, $F_{z\mathrm{CG}}$, and z_{m} in the small bending regime given by Eq. (9). Further details are found in Sec. III.

In order to check for finite size effects, we used several different sizes for the simulation box L_x, while L_y and L_z are kept small. The initial configurations of the DMPC bilayer systems are prepared by replicating a small system of 6.3 nm × 6.3 nm × 9.0 nm. The small membrane system consists of 128 DMPC lipids and 2128 CG water particles and was equilibrated in the NPT ensemble. The pressures normal and lateral to the membrane were separately controlled at 1.0 atm using a Parrinello-Rahman barostat[29] with a time constant of 5.0 ps. The temperature was set to 310 K using a Nosé-Hoover thermostat[32] with a time constant of 0.5 ps. The simulation box was elongated by copying the small system to obtain $L/L_y = 1$, 2, 3, 4, 5, and 6. We refer to these systems as S1, S2, S3, S4, S5, and S6, respectively. The total arc length of membrane, L, is chosen as L_x of the initially prepared planar membrane for each system. Thus, the area of the whole membrane is $S = LL_y$. Then, we introduced the cylinders into these systems, as shown in Fig. 1. In the MD simulations, L_y is kept constant, while L_x and L_z separately fluctuate to realize $\langle P_x\rangle = \langle P_z\rangle = 1$ atm. Namely, the MD simulations are carried out in the $\mathrm{NP}_x L_y \mathrm{P}_z \mathrm{T}$ ensemble. This is a reasonable choice to achieve a tensionless membrane as long as the membrane curvature is not too large. The settings for the thermostat and barostat are the same as for the equilibration runs of the small system. We measured the force of Eq. (22) in the range of $0 < z_{\mathrm{m}}/(L/4) < 0.5$. A time step of 10 fs is used. The nonbonded interaction is truncated at 1.5 nm, while the Coulomb interaction is computed using the Particle-Particle Particle-Mesh (PPPM) scheme.[33] MD simulation lengths were 100 ns (20 ns for equilibration) for the small systems, S1–S3, and 1 μs (200 ns for equilibration) for the larger systems, S4–S6, respectively. CG-MD simulations have been performed using the LAMMPS code.[34]

B. Calculation of bending rigidity by other methods for comparison

For the purpose of comparison, we also used the spectrum of thermal fluctuations of height and lipid orientation, and the lateral compression method to evaluate κ in the MD simulations using the same CG force field.[30,31] We briefly describe the simulation conditions and analysis methods here.

1. Height fluctuation spectrum

We have carried out a MD simulation of a DMPC bilayer for 1 μs. The system is composed of 2048 DMPC molecules and 34 048 CG water particles, which is the same hydration number as used in the MD simulations with the external cylinder potential. The statistical error is estimated using 10 independent samples by analyzing the spectrum in blocks of 100 ns. The glycerol "GL" segment of each DMPC molecule is used to define the membrane surface.[31] Since no flip-flop motion was detected during the simulations, the upper and lower leaflets of the membrane were clearly identified. A grid of 32 × 32 points was assigned to each monolayer giving one lipid molecule per grid point on average. When multiple lipids were found in a given grid cell, the height of the monolayer surface was calculated as an arithmetic average of the heights of the GL segments in the grid cell. When no lipids occupied a grid cell, the height of the grid cell was calculated as the arithmetic average of its neighbors. No smoothing filter to average over grid cells was used. The membrane height, h, at each grid point was taken as the average of the heights of the two monolayer surfaces. κ was then estimated from Eq. (2).

2. Spectrum of lipid orientation fluctuations

Using the theoretical notation derived in Ref. 22, the bending elasticity is related to fluctuations of lipid orientation:

$$\left\langle \left| n_q^{\parallel} \right|^2 \right\rangle = \frac{k_B T}{q^2 \kappa}, \tag{24}$$

where $n_q^{\parallel}$ is the longitudinal component of the spectrum of lipid orientation. The analysis has been made for the same MD trajectory of a DMPC bilayer system as used in the height fluctuation spectrum. The molecular orientation of a lipid was represented by the vector connecting from the midpoint of two ester segments "EST" towards the midpoint of the tail segments "CT." The notation of the segment is the same as in Ref. 31.

3. Buckling due to lateral compression

κ can also be estimated from the buckling of a membrane due to lateral compression.[25,26] The direction of the buckling is controlled by choosing the box size as $L_y < L_x$, which induces the buckling selectively along the x-axis. The membrane is laterally compressed by shrinking the L_x box size. Like the novel method proposed in this study, this method also induces membrane bending under PBC, and evaluates the bending rigidity by measuring the force required for the bending:

$$F_x = L_y L_z (P_x - P_z). \tag{25}$$

MD simulations have been repeated at different cell lengths L_x. The projected area on the x–y plane, $A = L_x L_y$, is constant during the MD simulations; thus, the NP_zAT ensemble is employed. A Parrinello-Rahman barostat[29] and Nosé-Hoover thermostat[32] are used to realize the conditions $P_z = 1$ atm and $T = 310$ K. We used system S4 for this study. L_x was varied over nine different lengths in the range of $0.6 < L_x/L < 1$. The simulation length was 1 μs for each choice of L_x.

III. RESULTS AND DISCUSSION

A. Numerical simulation of the discretized Helfrich model

We now report the results from LD simulations of the discrete particle model derived from the Helfrich model. In this model, the membrane is represented by n discretized particles, and the constant area condition is approximated with a harmonic spring of force constant $k^*_{\rm bond}$. In the limit of large n and $k^*_{\rm bond}$, the discretized model is equal to the Helfrich model. Figure 3(a) shows convergence of the force $F_{z\rm H}$ with increasing n, where $k^*_{\rm bond} = 6.4 \times 10^4$. For any choice of z_m, the force is well converged at $n = 64$; the relative error of the force is less than 0.3% at $n = 64$ with respect to the force at $n = 256$. Figure 3(b) shows convergence of the force $F_{z\rm H}$ with increasing $k^*_{\rm bond}$, where $n = 64$. $k^*_{\rm bond} = 6.4 \times 10^4$ is large enough to obtain the converged force; the relative error is less than 0.3% with respect to the force obtained with $k^*_{\rm bond} = 6.4 \times 10^5$. The convergence of $F_{z\rm H}$ is not affected by the system size or κ.

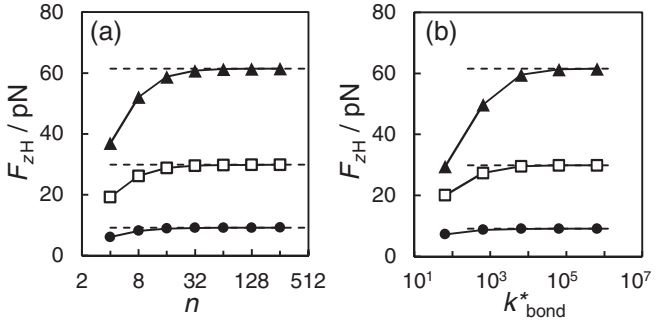

FIG. 3. Convergence of $F_{z\rm H}$ as a function of the number of bead segments, n (a), and bond potential strength, $k^*_{\rm bond}$ (b), of the discretized Helfrich model. The results are obtained for the system $L/L_y = 4$ and $\kappa = 9.5 \times 10^{-20}$ J. The forces are calculated at $z_{\rm m}/L = 0.025$ (filled circles), 0.075 (open squares), and 0.125 (filled triangles).

Thus, we use $n = 64$ and $k^*_{\rm bond} = 6.4 \times 10^4$ for all LD simulations of the discretized Helfrich model.

Figure 4(a) plots the average force $F_{z\rm H}$ as a function of the bending rigidity κ. It is clearly seen that the force $F_{z\rm H}$ is proportional to the bending rigidity κ. This relation is useful as a reference to estimate the bending rigidity of a membrane described by a molecular model on the basis of measuring the force $F_{z\rm CG}$.

Figure 4(b) plots the force $F_{z\rm H}$ as a function of the contacting height $z_{\rm m}$ of the cylinder to the membrane surface. LD was usually conducted at a finite temperature of 310 K, although we also estimated the force at $T = 0$ K using simulated annealing. The slope of the force for $z_{\rm m} < 1$ nm at $T = 0$ K shows good agreement with the theoretical force of Eq. (9) derived in the small bending regime. Thus, we confirmed that the simulation of the discretized Helfrich model correctly reproduces the mechanical properties of the Helfrich membrane at $T = 0$ K. The LD simulations at $T = 310$ K reveal that the force is increased by the thermal fluctuations of the membrane surface, which is more important at small $z_{\rm m}$ heights. Since the increment of $F_{z\rm H}$ due to thermal fluctuations directly affects the estimation of the bending rigidity, it is important to take into account the thermal fluctuations using a numerical simulation.

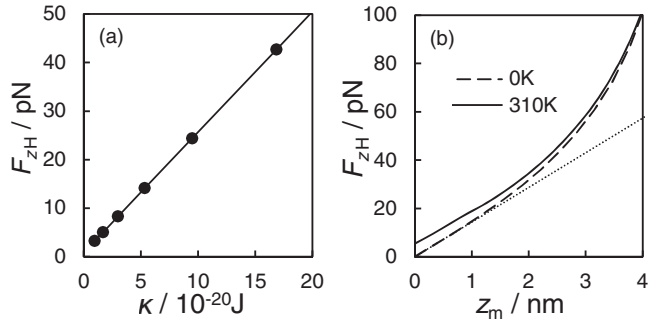

FIG. 4. Average force exerted on the curved membrane from the supporting cylinders in the LD simulation of the discretized Helfrich model. The results are obtained for the system $L/L_y = 4$. (a) The force $F_{z\rm H}$ as a function of the bending rigidity κ for the contacting position $z_{\rm m} = 1.3$ nm and the temperature $T = 310$ K. (b) The force $F_{z\rm H}$ as a function of $z_{\rm m}$ at $T = 310$ K (solid line) and $T = 0$ K (dashed line) for $\kappa = 9.5 \times 10^{-20}$ J. The theoretical slope of Eq. (9) derived in the limit of $z_{\rm m} \ll L$ is also plotted (dotted line).

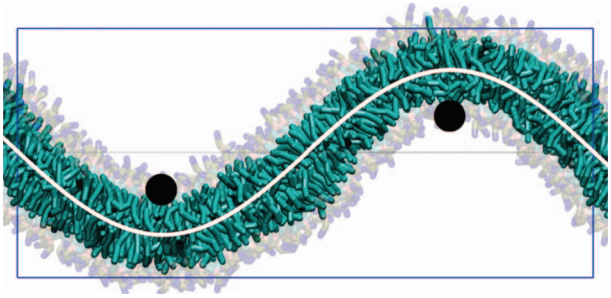

FIG. 5. A snapshot from a CG-MD simulation of a DMPC membrane (S4) at $z_{cyl} = 1.4$ nm. Cylindrical repulsive walls (black circles) push on the lipid hydrophobic tails (cyan). Lipid head groups are shown translucence and water particles are not shown for simplicity. The simulation unit cell is drawn with thin blue lines. The white line denotes the ideal curved membrane profile of the Helfrich model at the same z_m value.

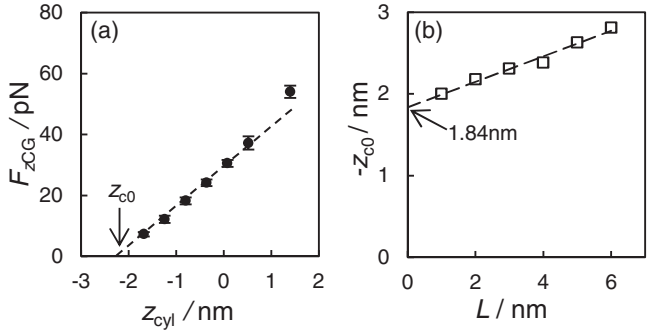

FIG. 6. (a) The force F_{zCG} as a function of the cylinder position z_{cyl} obtained from CG-MD of the system S4. The fit to the data is shown with a dashed line. z_{c0} is identified as the zero force value of the fit. (b) z_{c0} is plotted as a function of the membrane size L. A linear fit is shown with a dashed line.

B. Bending rigidity from CG-MD simulations of a DMPC bilayer

Figure 5 shows a typical snapshot from a CG-MD simulation of a DMPC bilayer in the presence of two cylindrical wall potentials. The cylinders repel the hydrophobic core of the membrane, thus imposing a sinusoidal deformation on the membrane. The ideal curved membrane profile derived from the Helfrich model at the same z_m is also plotted in white. The Helfrich profile is close to the mid-plane of the lipid bilayer, which suggests that the bilayer system behaves as predicted by the Helfrich model.

Different from the Helfrich model, the actual membrane simulated by CG-MD has a finite thickness. We need to estimate the membrane thickness, d, to clearly define the membrane height at the contact line to the cylinder, z_m, using Eq. (23). We plot the force F_{zCG} measured at several cylinder positions, z_{cyl}, for a DMPC bilayer of $L = 25.2$ nm (S4) in Fig. 6(a). The average force is well converged during the MD run as seen from the small error bars estimated by block analysis. In the small bending limit, i.e., $z_m \ll L$, the force F_{zCG} should be a linear function of z_m, and thus of z_{cyl}, according to Eq. (9). This is clearly confirmed from Fig. 6(a). We obtain the straight line by a least-squares fit using the first three points in the small z_{cyl} regime. Then, we estimate the coordinate of z_{c0}, which is the cylinder position which contacts the membrane. Since the CG-MD simulations have been carried out at finite temperature, z_{c0} is affected by the undulations of the membrane. The amplitude of undulation, h, is related to the size of the membrane as $h \sim L$.[14] Therefore, z_{c0} estimated from different box sizes are different as shown in Fig. 6(b). Taking the limit of $L \to 0$, we evaluate the position of the cylinder that first contacts the membrane with no undulations, where $z_m = 0$ by definition. We obtained $z_{c0,\,L\to 0} = -1.84$ nm, and, using Eq. (23), $d = 2.48$ nm from $0 = z_{c0,\,L\to 0} + R_0 + d/2$.

Figure 7 shows the force F_{zCG} as a function of z_m. We evaluate the bending rigidity from each force F_{zCG} by assuming $F_{zCG} = F_{zH}(\kappa)$ that we evaluated using the discretized Helfrich model at the same conditions for L, L_y, T, and z_m. The obtained κ is also plotted in Fig. 7. κ is almost constant over all z_m. The convergence of κ seems better at larger z_m, although the approximation made in the Helfrich model degrades, in principle, for a highly curved membrane. For example, higher order elastic energy terms should affect the force. Therefore, we typically estimate κ using the force for $0 < z_m/(L/4) < 0.5$, which is $0 < z_m < 3$ nm for system S4. Taking the average in the range of $0 < z_m < 3$ nm, we obtain $\kappa = (8.6 \pm 0.4) \times 10^{-20}$ J, which is plotted as a dotted line in Fig. 7. We also plot the force curve of F_{zH} using $\kappa = 8.6 \times 10^{-20}$ J as a solid line in the figure.

A finite size effect on the value of κ in the present method is examined. Figure 8 plots the estimated κ as a function of membrane size, L. For a small membrane patch, the membrane cannot ideally deform in the presence of the two cylinders as assumed in the Helfrich model. Since the force required to repel the membrane is larger for a smaller membrane patch, the cylinder induced a local structural relaxation of the lipids around the cylinders in the smaller systems. Therefore, the estimated κ shows a membrane size dependency for small membranes ($L \lesssim 20$ nm). The method is safely used for a large membrane patch, where the approximation in the Helfrich model is reasonable such that the membrane thickness is negligible compared with L. The bending rigidity converges to a constant value for large membrane sizes $L > 25$ nm (Fig. 8). The minimum size required for the convergence should be determined by the elastic properties of

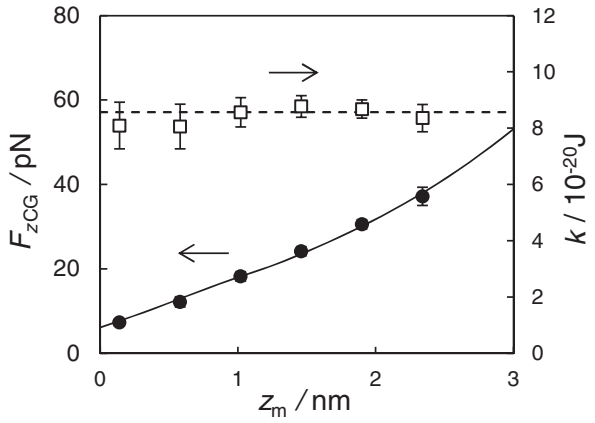

FIG. 7. The force F_{zCG} (solid circles) exerted on the membrane from the supporting cylinders and the bending rigidity κ (open squares) of the DMPC bilayer of system S4 as a function of z_m. The solid line is the fitting function of the force derived from the Helfrich model with $\kappa = 8.6 \times 10^{-20}$ J.

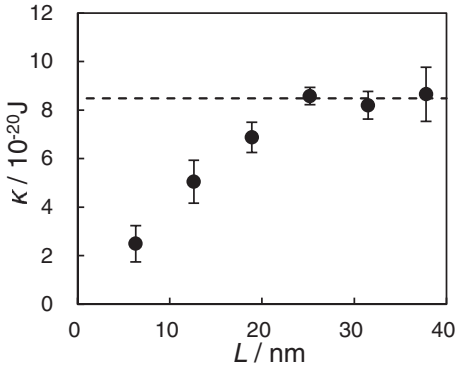

FIG. 8. Estimated bending rigidity κ from CG-MD of a DMPC bilayer as a function of the membrane size, L.

the membrane. Therefore, assuming similar elastic properties, the minimum size would be the same for all-atom MD ($N_{\text{lipid}} \sim 512$). This is smaller than that typically used in the analysis of the height fluctuation spectrum (e.g., $N_{\text{lipid}} \sim 2048$). Therefore, the present method should be useful for all-atom MD simulations. By averaging over $L > 25$ nm, we obtain $\kappa = (8.6 \pm 0.4) \times 10^{-20}$ J for the DMPC bilayer. The reported experimental values of κ for DMPC membranes are in the wide range of 2.9–13 $\times 10^{-20}$ J,[35–39] though the most probable value is around 10×10^{-20} J, which is similar to our estimation of κ by the present method. The large uncertainty may be related to the different methods used in the experimental measurements.[39]

C. Comparison with other methods

1. Height fluctuation spectrum

Figure 9 plots the height fluctuation spectrum $\langle |h_q|^2 \rangle$ of the DMPC bilayer. The solid line shows the fitting function of Eq. (2) derived from the Helfrich model with $\kappa = 8.6 \times 10^{-20}$ J, which is obtained by a least-squares fit of the smallest four q points (i.e., $q_{\text{cut}} = 0.56$ nm^{-1}). Thus, the κ value is the same as obtained by the proposed method. However, the difficulty is its sensitivity to the choice of fitting parameters, especially q_{cut}.[20] We found that κ gradually decreases with increasing q_{cut}. For example, if we use the smallest seven points in the plot ($q_{\text{cut}} = 0.79$ nm^{-1}), we obtain $\kappa = 6.9 \times 10^{-20}$ J, which is the same value as found in a previous paper[31] using a different fitting function proposed by Brannigan and Brown.[21] The latter function has been derived from the extended continuous model,[21] which includes deformations of a lipid bilayer such as protrusions, peristaltic modes, and area expansion. The function uses a wider range of q values for the fitting ($q_{\text{cut}} = 3.0$ nm^{-1}). The fitting function is also presented as a dashed line in Fig. 9. The data points are dense in the high-q range so that the fitting is weighted more heavily in the high-q data. Unfortunately the agreement of the fitting curve degrades in the important low-q range. Thus, it is difficult to determine which is a more appropriate estimate for κ from Fig. 9. Namely, there is ambiguity in the fitting procedure in this analysis. Nonetheless, it was confirmed that the proposed method yields a consistent κ value with those estimated by a conventional height fluctuation spectrum within fitting error.

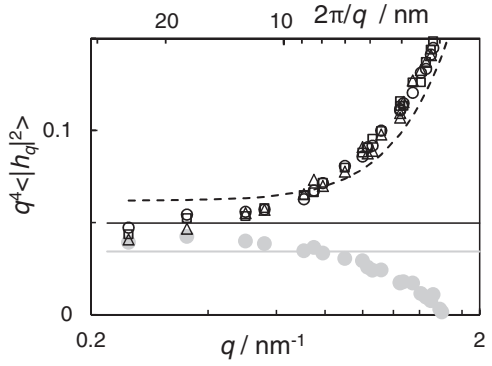

FIG. 9. The height fluctuation spectrum $\langle |h_q|^2 \rangle$ of the DMPC bilayer multiplied by q^4 (open circles, triangles, and squares are obtained from three different 1 μs MD runs, respectively). The dashed line is the fitting function derived from the extended continuous model[21] with $\kappa = 6.9 \times 10^{-20}$ J. The solid and gray lines are the function of Eq. (2) with $\kappa = 8.6 \times 10^{-20}$ J (as measured by the guiding method) and $\kappa = 12.5 \times 10^{-20}$ J (as measured by the spectrum of longitudinal lipid orientation fluctuations). The filled circles in gray represent the modified height fluctuation spectrum by subtracting the tilt energy contribution.[22]

2. Spectrum of lipid orientation fluctuations

The spectrum of longitudinal lipid orientation fluctuations shows a good convergence to the power law of Eq. (24) in the wider q range, as shown in Fig. 10. The dashed fitting line was obtained by a linear least-squares fitting of the smallest seven q points (i.e., $q_{\text{cut}} = 0.79$ nm^{-1}); namely, using data points of the wavelengths greater than twice the membrane thickness. It was obvious that the fit was significantly improved. The obtained bending rigidity from this fit is 12.5×10^{-20} J, which is larger than the estimate from the height fluctuation spectrum. The model used in the analysis includes an additional tilt energy contribution, $k_{\text{B}}T/K_\theta q^2$ (K_θ is the tilt modulus), to the height fluctuation spectrum.[22] We also evaluate the tilt modulus from the transverse orientation spectrum. The modified height fluctuation spectrum obtained by subtracting the tilt energy contribution is also plotted as

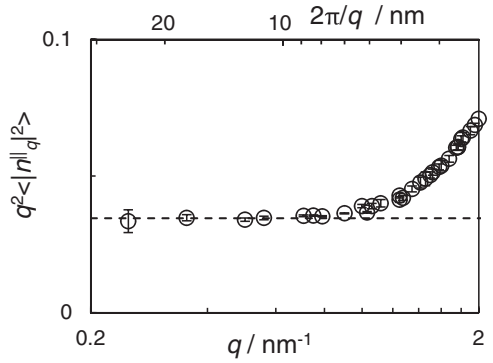

FIG. 10. The spectrum of longitudinal lipid orientation fluctuations $\langle |n_q^{\parallel}|^2 \rangle$ of the DMPC bilayer multiplied by q^2. The dashed line is the fitting function of Eq. (24) with $\kappa = 12.5 \times 10^{-20}$ J.

gray circles in Fig. 9. This yields a κ value of 10.7×10^{-20} J using the smallest four q points.

Figure 9 reveals that the tilt energy contribution is negligible only at the smallest q ($L \sim 25$ nm). The length of 25 nm corresponds to the minimum membrane size required to see the convergence of κ by the proposed guiding method (see Fig. 8). Thus, the size dependency found in the κ values by the guiding method for a small membrane patch may be explained by the tilt energy contribution. This may suggest that a larger system is required to estimate κ using Eq. (2) from the height fluctuation spectrum as pointed out previously.[22] However, the convergence of the height fluctuation spectrum at the smallest two q points is not good even with 1 μs MD trajectories (see the difference in Fig. 9 between the data corresponding to three separate 1 μs MD trajectories). A full understanding of the origin of the quantitative discrepancy will need further study with longer MD simulations of larger membrane systems, which is beyond the scope of the present paper.

3. Buckling due to lateral compression

We also evaluated the bending rigidity using the lateral compression method.[25,26] For this method, we measured the lateral compression force required for buckling and obtained κ using an analytic expression for the force derived by Noguchi.[26] Figure 11 plots the compression force $F_{x\mathrm{CG}}$ of the DMPC bilayer as a function of $\Delta L_x = L - L_x$, the decrease of the cell length L_x from that of the tensionless planar membrane due to the lateral compression of the membrane along the x-axis. Under small compression, i.e., $\Delta L_x < 2$ nm, the membrane stays planar with a shrinking surface area. The forces in this range are not useful to estimate the bending rigidity. Upon further increasing the compression, the membrane started to buckle. κ is evaluated from the lateral force to support the buckled membrane and is plotted in Fig. 11. The obtained κ values are constant over the range of $2 < \Delta L_x < 10$ nm within statistical error. Thus, we obtain $\kappa = (9.7 \pm 0.4) \times 10^{-20}$ J from this method. This is larger than that obtained from the guiding potential method by $13\% \pm 6\%$. The lateral compression decreases the membrane area and increases the membrane thickness. In the case of system S4, the membrane thickness, D, of the DMPC bilayer was increased by $\Delta D/D = 4\%$. Using a relation predicted by polymer brush theory,[4] $\kappa = K_A D^2/24$, where K_A is the area expansion modulus, we can estimate the increase of κ by the lateral compression as $\Delta\kappa/\kappa \sim 2\Delta D/D = 8\%$. Thus, the higher κ value obtained using the lateral compression method can be rationalized by the increase in membrane thickness. When K_A is large, the increase in membrane thickness should be negligible assuming a constant volume of the membrane. In this limit, the lateral compression method should yield a similar κ value as measured by the guiding potential method.

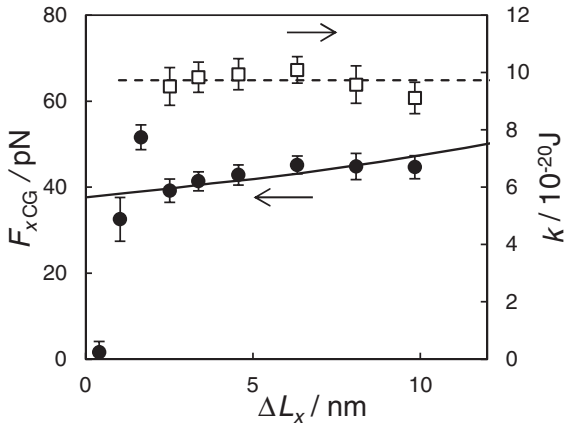

FIG. 11. The force $F_{x\mathrm{CG}}$ (filled circles) to support the compressed membrane and the calculated bending rigidity κ (open squares) of the DMPC bilayer of system S4 as a function of the box length, $\Delta L_x (= L - L_x)$. Each bending rigidity value is calculated from the force measured at the given value of ΔL_x. The solid line is the fitting function of the force derived from the Helfrich model with $\kappa = 9.7 \times 10^{-20}$ J.

IV. CONCLUSIONS

We presented a new method for estimating the bending rigidity of a lipid bilayer from MD simulations by imposing membrane bending using two symmetrically placed cylindrical external guiding potentials. The method relies on reference data of the required force to support the curved membrane, which is obtained from a discretized Helfrich model using a Langevin dynamics simulation. The discretized Helfrich model is needed to bridge the molecular system and the continuum representation of the Helfrich model. The Helfrich model is solved numerically, instead of using an analytic small gradient approximation as was done previously.[27] The Langevin dynamics simulation can evaluate the force induced not only by the bending energy but also due to thermal fluctuations, which is important to accurately estimate the bending rigidity. We employed the present method in CG-MD simulations of a DMPC membrane and obtained a reasonable bending rigidity for large membrane sizes of $L > 25$ nm. The κ value is consistent with that obtained from thermal fluctuations of the membrane height of a tension-free membrane within the fitting errors. An estimate of bending rigidity from thermal fluctuations of lipid orientation gave a higher value than those obtained by other simulation methods, though such a difference has also been observed among the different methods of experimental measurements.[39] The bending rigidity obtained from the lateral compression force required to support a buckled membrane seems to be slightly higher than that of the tension-free membrane; the difference was explained due to the slight compression. The present method gives a practical procedure for the estimation of the bending rigidity of realistic lipid bilayers based on active deformation of the membrane.

ACKNOWLEDGMENTS

We thank Professor Noguchi for helpful discussion. This work is supported by JSPS KAKENHI Grant No. 23350014, the Next Generation Super Computing Project, TCCI/CMSI in the Strategic Programs for Innovative Research, MEXT, Japan, and HPCI Systems Research Projects (Project ID hp120093).

[1]W. Helfrich, Z. Naturforsch. C **28**, 693 (1973).
[2]Z. Chen and R. P. Rand, Biophys. J. **73**, 267 (1997).
[3]R. S. Gracia, N. Bezlyepkina, R. L. Knorr, R. Lipowsky, and R. Dimova, Soft Matter **6**, 1472 (2010).
[4]W. Rawicz, K. C. Olbrich, T. McIntosh, D. Needham, and E. Evans, Biophys. J. **79**, 328 (2000).
[5]S. Tristram-Nagle and J. F. Nagle, Biophys. J. **93**, 2048 (2007).
[6]M. Hu, J. J. Briguglio, and M. Deserno, Biophys. J. **102**, 1403 (2012).
[7]D. Sengupta, J. Phys. Chem. B **116**, 14556 (2012).
[8]M. Orsi, D. Y. Haubertin, W. E. Sanderson, and J. W. Essex, J. Phys. Chem. B **112**, 802 (2008).
[9]S. Baoukina, S. J. Marrink, and D. P. Tieleman, Faraday Discuss. **144**, 393 (2010).
[10]S. J. Marrink, H. J. Risselada, S. Yefimov, D. P. Tieleman, and A. H. de Vries, J. Phys. Chem. B **111**, 7812 (2007).
[11]T. Nakamura, W. Shinoda, and T. Ikeshoji, J. Chem. Phys. **135**, 094106 (2011).
[12]T. Nakamura and W. Shinoda, J. Chem. Phys. **138**, 124903 (2013).
[13]R. Goetz, G. Gompper, and R. Lipowsky, Phys. Rev. Lett. **82**, 221 (1999).
[14]E. Lindahl and O. Edholm, Biophys. J. **79**, 426 (2000).
[15]G. Brannigan, L. Lin, and F. Brown, Eur. Biophys. J. **35**, 104 (2006).
[16]G. Brannigan, A. C. Tamboli, and F. L. Brown, J. Chem. Phys. **121**, 3259 (2004).
[17]S. J. Marrink and A. E. Mark, J. Phys. Chem. B **105**, 6122 (2001).
[18]M. J. Stevens, J. Chem. Phys. **121**, 11942 (2004).
[19]I. R. Cooke, K. Kremer, and M. Deserno, Phys. Rev. E **72**, 011506 (2005).
[20]H. Shiba and H. Noguchi, Phys. Rev. E **84**, 031926 (2011).
[21]G. Brannigan and F. L. H. Brown, Biophys. J. **90**, 1501 (2006).
[22]M. C. Watson, E. G. Brandt, P. M. Welch, and F. L. H. Brown, Phys. Rev. Lett. **109**, 028102 (2012).
[23]O. Farago and P. Pincus, J. Chem. Phys. **120**, 2934 (2004).
[24]V. A. Harmandaris and M. Deserno, J. Chem. Phys. **125**, 204905 (2006).
[25]W. K. den Otter, J. Chem. Phys. **123**, 214906 (2005).
[26]H. Noguchi, Phys. Rev. E **83**, 061919 (2011).
[27]W. K. den Otter and W. J. Briels, J. Chem. Phys. **118**, 4712 (2003).
[28]J. P. Ryckaert, G. Ciccotti, and H. J. C. Berendsen, J. Comput. Phys. **23**, 327 (1977).
[29]M. Parrinello and A. Rahman, Phys. Rev. Lett. **45**, 1196 (1980).
[30]W. Shinoda, R. DeVane, and M. L. Klein, Mol. Simul. **33**, 27 (2007).
[31]W. Shinoda, R. DeVane, and M. L. Klein, J. Phys. Chem. B **114**, 6836 (2010).
[32]D. J. Evans and B. L. Holian, J. Chem. Phys. **83**, 4069 (1985).
[33]D. Frenkel and B. Smit, *Understanding of Molecular Simulation*, 2nd ed. (Academic Press, 2002).
[34]S. J. Plimpton, J. Comput. Phys. **117**, 1 (1995).
[35]T. Salditt, M. Vogel, and W. Fenzl, Phys. Rev. Lett. **93**, 169903 (2004).
[36]N. Kucerka, Y. Liu, N. Chu, H. I. Petrache, S. Tristram-Nagle, and J. F. Nagle, Biophys. J. **88**, 2626 (2005).
[37]P. Meleard, C. Gerbeaud, T. Pott, L. Fernandez-Puente, I. Bivas, M. D. Mitov, J. Dufourcq, and P. Bothorel, Biophys. J. **72**, 2616 (1997).
[38]C.-H. Lee, W.-C. Lin, and J. Wang, Phys. Rev. E **64**, 020901 (2001).
[39]J. F. Nagle, Faraday Discuss. **161**, 11 (2013).